



## 4-(1,3-Thiazol-2-yl)morpholine derivatives as inhibitors of phosphoinositide 3-kinase

Rikki Alexander<sup>a,\*</sup>, Ahrani Balasundaram<sup>a</sup>, Mark Batchelor<sup>a</sup>, Daniel Brookings<sup>a</sup>, Karen Crépy<sup>a</sup>, Tom Crabbe<sup>b</sup>, Marie-France Deltent<sup>c</sup>, Frank Driessens<sup>c</sup>, Andrew Gill<sup>b</sup>, Sue Harris<sup>d</sup>, Gillian Hutchinson<sup>b</sup>, Claire Kulisa<sup>a</sup>, Mark Merriman<sup>b</sup>, Prakash Mistry<sup>d</sup>, Ted Parton<sup>e</sup>, James Turner<sup>a</sup>, Ian Whitcombe<sup>a</sup>, Sara Wright<sup>e</sup>

<sup>a</sup> Department of Medicinal Chemistry, UCB, 208 Bath Road, Slough, Berkshire SL1 3WE, UK

<sup>b</sup> Department of Biology, UCB, 208 Bath Road, Slough, Berkshire SL1 3WE, UK

<sup>c</sup> CPR&ES, UCB Pharma SA, Chemin du Foriest, 1420 Braine-l'Alleud, Belgium

<sup>d</sup> Department of Pharmacology, UCB, 208 Bath Road, Slough, Berkshire SL1 3WE, UK

<sup>e</sup> Department of DMPK, UCB, 208 Bath Road, Slough, Berkshire SL1 3WE, UK

### ARTICLE INFO

#### Article history:

Received 16 May 2008

Revised 23 June 2008

Accepted 25 June 2008

Available online 28 June 2008

#### Keywords:

PI3K

Oncology

Kinase inhibitor

### ABSTRACT

4-(1,3-Thiazol-2-yl)morpholine derivatives have been identified as potent and selective inhibitors of phosphoinositide 3-kinase. The SAR data of selected examples are presented and the in vivo profiling of compound **18** is shown to demonstrate the utility of this class of compounds in xenograft models of tumor growth.

© 2008 Elsevier Ltd. All rights reserved.

The phosphoinositide 3-kinase (PI3K) family consists of eight catalytic proteins, divided into three subclasses, Class I, Class II, and Class III.<sup>1</sup> The Class I subclass is further divided into Class Ia ( $\alpha$ ,  $\beta$ , and  $\delta$  isoforms) and Class Ib ( $\gamma$  isoform). They are activated by growth factor receptor activation (Class Ia) or GPCRs (Class Ib) and then catalyze the phosphorylation of phosphatidylinositol-4,5-bisphosphonate (PIP2) to phosphatidylinositol-3,4,5-trisphosphonate (PIP3) which acts as a second messenger. The PI3K pathway is implicated in a variety of physiological functions that are known to be involved in the pathology of cancer, metabolic, inflammatory,<sup>2</sup> and cardiovascular diseases.<sup>3</sup> Aberrant upregulation of the PI3K pathway is implicated in a wide variety of human cancers.<sup>4</sup> In particular, mutations in the PI3K $\alpha$  gene, which confer oncogenicity and lead to constitutive kinase activity, have been identified in many cancers. The PTEN tumor suppressor gene is a phosphoinositide 3-phosphatase that converts PIP3 into PIP2 and, therefore, downregulates pathways that are PIP3 dependent; deletion of this enzyme leads to activation of the PI3K pathway and oncogenicity.<sup>5</sup> We report in this Letter our initial efforts to identify

novel inhibitors of PI3K Class I that demonstrate activity against cancer cell lines.

A Catalyst hybrid shape/feature pharmacophore was generated using WebLab Viewer Pro, Version 4.2 (Accelrys Software Inc., San Diego, CA), based on a published X-ray crystal structure of LY294002<sup>6</sup> bound to PI3K $\gamma$  (PDB ID: 1E7V).<sup>7</sup> The pharmacophore comprised a ligand shape query feature, combined with two hydrogen bond acceptor features; the latter aligned to the ligand lone pair vectors that best corresponded to the direction of the respective protein acceptor hydrogen atoms, the amide NH of Val882 and the NH of the side chain of Lys833. Location spheres of 1.5 Å radius were added to constrain both the hydrogen bond acceptor and donor locations (Fig. 1). The pharmacophore was used to search commercial drug-like compound databases using Catalyst, Version 4.6 (Accelrys Software Inc., San Diego, CA.). A number of virtual 'hits' were obtained, which were validated in a biochemical screen.<sup>8</sup> Compound **1** was identified as a compound of interest due to its good ligand efficiency<sup>9</sup> of 0.42 kcal mol<sup>-1</sup> against PI3K $\gamma$  and synthetic tractability (Fig. 2). Compound **1** showed comparable activity against PI3K isoforms (Table 1) compared with LY294002 (IC<sub>50</sub> = 975, 1713, 1025, and 10050 nM for  $\alpha$ ,  $\beta$ ,  $\delta$ , and  $\gamma$ , respectively) and was inactive against a panel of kinases that included AKT (data not shown).

\* Corresponding author. Tel.: +44 (0)1753 534655; fax: +44 (0)1753 536632.  
E-mail address: [rikki.alexander@ucb-group.com](mailto:rikki.alexander@ucb-group.com) (R. Alexander).

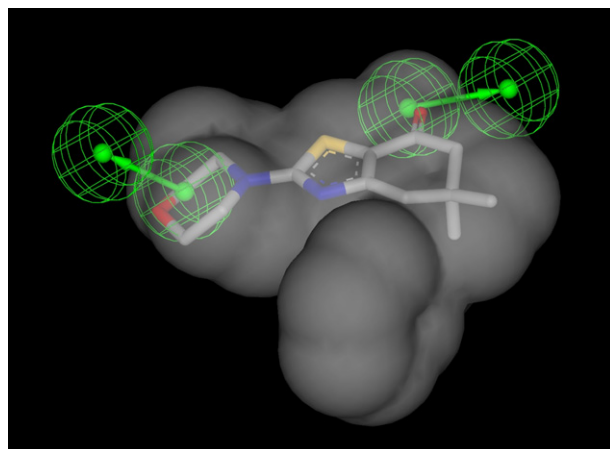


**Figure 1.** Catalyst pharmacophore generated with WebLab Viewer Pro, Version 4.2 (Accelrys Software Inc., San Diego, CA), showing ligand shape descriptor (grey shape) and two hydrogen bond acceptor features described in the text (green vectors and spheres). The 'hit' molecule **1** is shown in the alignment 'found' by Catalyst.

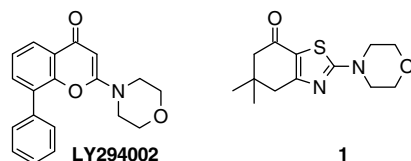
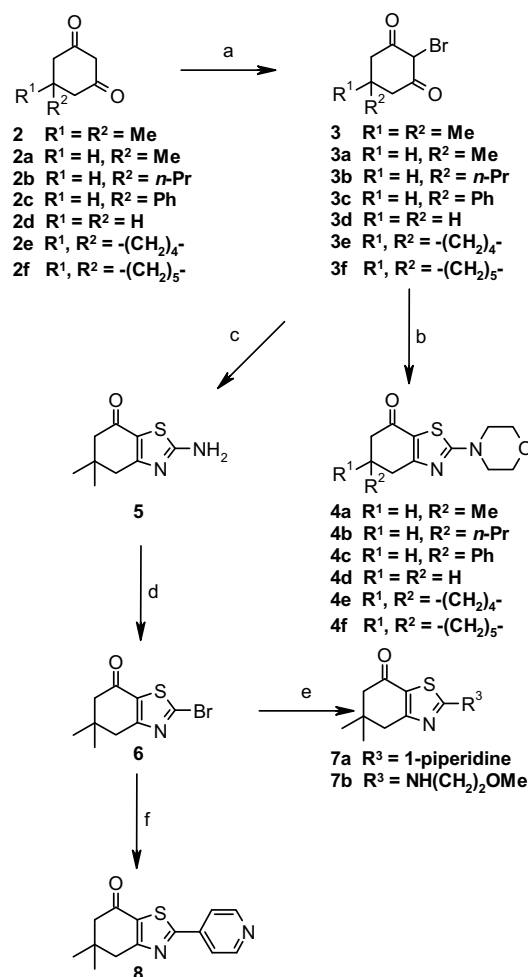


**Figure 2.** LY294002 and screening hit, compound **1**.

Analogues of compound **1** were synthesized by the methods<sup>8</sup> outlined in Scheme 1 to elucidate the basic SAR, shown in Table 1. Bromination of the readily available cyclic 1,3-diketones **2–2f** gave the bromide **3–3f** in good to poor yields as a single regioisomer. Compounds **3a–3f** were reacted with 4-morpholine carbothioamide to give compounds **4a–4f** in yields ranging from 7% to 60%. Reaction of compound **3** with thiourea yielded compound **5** in 73% yield. Compound **5** was converted via diazotization to the bromide, compound **6** in 74% yield. This could be elaborated by either nucleophilic displacement of the bromide to give compounds **7a** (82% yield) and **7b** (76% yield) or by palladium mediated coupling to yield compound **8** in 33% yield.

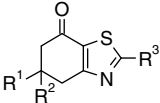
As shown in Table 1, the dimethyl substitution was optimal. Removal of the methyl groups led to a loss in activity (compound **4d**). Replacing the methyl group in compound **4a** with a propyl, com-



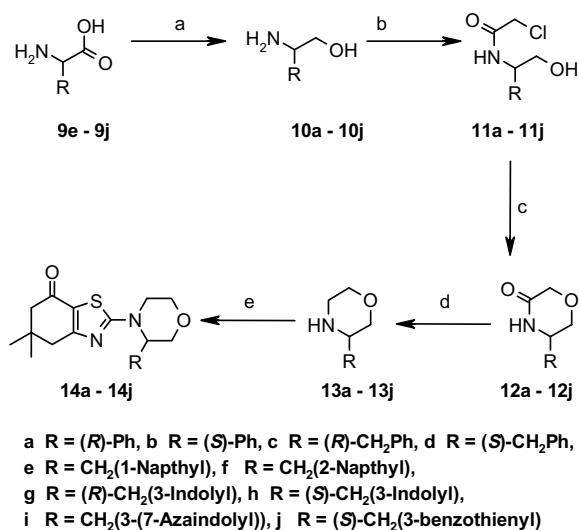
**Scheme 1.** Reagents and conditions: (a) Br<sub>2</sub>, AcOH, rt, **3** 98%, **3a** 99%, **3b** 99%, **3c** 100%, **3d** 100%, **3e** 29%, **3f** 99%; (b) 4-morpholine carbothioamide, *i*-Pr<sub>2</sub>NEt, THF, reflux, **4a** 19%, **4b** 20%, **4c** 60%, **4d** 28%, **4e** 7%, **4f** 34%; (c) H<sub>2</sub>NCSNH<sub>2</sub>, *i*-Pr<sub>2</sub>NEt, THF, reflux, 73%; (d) CuBr<sub>2</sub>, *t*-BuONO, MeCN, 25 °C, 74%; (e) nucleophile, *i*-Pr<sub>2</sub>NEt, *i*-PrOH, reflux, **7a** 82%, **7b** 76%; (f) 4-PyB(OH)<sub>2</sub>, Pd(Ph<sub>3</sub>P)<sub>4</sub>, 1,4-dioxane, Na<sub>2</sub>CO<sub>3</sub>, reflux, 33%.

pound **4b**, or phenyl group, compound **4c**, also led to a decrease in potency, suggesting a steric limitation. Spiro compounds **4e** and **4f** were tolerated, but offered no advantage. Replacement of the morpholine by piperidine, compound **7a**, led to a complete loss of activity, suggesting that the oxygen is making a key hydrogen

**Table 1**  
Exploratory SAR of initial hit: activity against PI3K isoforms<sup>8</sup>

Compound	R1, R2	R3				
			α	β	δ	γ
<b>1</b>	Me,Me	4-Morpholine	1333	693	701	3453
<b>4a</b>	Me,H	4-Morpholine	2494	4200	5973	16,700
<b>4b</b>	<i>n</i> -Pr,H	4-Morpholine	8393	11,460	26,240	19,790
<b>4c</b>	Ph,H	4-Morpholine	23,800	14,020	31,710	>40,000
<b>4d</b>	H,H	4-Morpholine	8063	3581	3887	16,670
<b>4e</b>	–(CH <sub>2</sub> ) <sub>4</sub> –	4-Morpholine	2429	1279	1482	16,060
<b>4f</b>	–(CH <sub>2</sub> ) <sub>5</sub> –	4-Morpholine	1900	1609	1176	6259
<b>7a</b>	Me,Me	1-Piperidine	>40,000	>40,000	>40,000	>40,000
<b>7b</b>	Me,Me	NH(CH <sub>2</sub> ) <sub>2</sub> OMe	>40,000	>40,000	>40,000	>40,000
<b>8</b>	Me,Me	4-Pyridine	20,280	4163	19,040	35,730

Values are means of two experiments. IC<sub>50</sub> is quoted in nM. Compounds **4a**, **4b**, and **4c** are racemic.



**Scheme 2.** Reagents and conditions: (a) BH<sub>3</sub>·Me<sub>2</sub>S, THF, reflux, **10e** 89%, **10f** 89%, **10g** 92%, **10h** 92%, **10i** 21%, **10j** 89%; (b) chloroacetyl chloride, Et<sub>3</sub>N, THF, 25 °C, **11a** 99%, **11b** 98%, **11c** 100%, **11d** 86%, **11e** 92%, **11f** 72%, **11g** 90%, **11h** 84%, **11i** 55%, **11j** 91%; (c) NaH, THF, 25 °C, **12a** 62%, **12b** 72%, **12c** 53%, **12d** 69%, **12e** 44%, **12f** 53%, **12g** 82%, **12h** 70%, **12i** 63%, **12j** 61%; (d) LiAlH<sub>4</sub>, THF, 25 °C, **13a** 22%, **13b** 54%, **13c** 13%, **13d** 81%, **13e** 64%, **13f** 74%, **13g** 89%, **13h** 67%, **13i** 8%, **13j** 84%; (e) **6**, *i*-Pr<sub>2</sub>NEt, *i*-PrOH, reflux, **14a** 5%, **14b** 12%, **14c** 27%, **14d** 84%, **14e** 76%, **14f** 83%, **14g** 47%, **14h** 88%, **14i**, 24%, **14j** 81%.

bond with the hinge region of the kinase, analogous to that made by LY294002 in PI3Kγ.<sup>7</sup> This interaction was one of the hydrogen bond acceptor features included in our pharmacophore. None of the modifications of compound **1** led to an isoform selective inhibitor, except replacement of the morpholine by 4-pyridyl, compound **8**, which led to a degree of PI3Kβ selectivity.

Molecular modeling suggested that it might be possible to increase potency through hydrophobic interactions with the residues on the edge of the ATP binding site. We sought to access these interactions by substituents at the 3 position of the morpholine ring. A range of 3-substituted morpholines were synthesized from either the amino acids, **9e–j**, or amino alcohols, **10a–d**, as outlined in Scheme 2. Amino acids **9e–j** were reduced to the amino alcohols **10e–j**. Amino alcohols **10a–j** were reacted with chloroacetyl chloride to give the amides **11a–j**. Cyclization under basic conditions gave the morpholinone **12a–j**. Reduction yielded the substituted morpholines **13a–j**. These were reacted with compound **6** to give compounds **14a–j**.

**Table 2**  
SAR of morpholine substituents: activity against PI3K isoforms<sup>8</sup>

Compound	R	Chirality	α	β	δ	γ
<b>1</b>	H		1333	693	701	3453
<b>14a</b>	Ph	<i>R</i>	>50,000	>50,000	>50,000	>50,000
<b>14b</b>	Ph	<i>S</i>	>50,000	>50,000	>50,000	>50,000
<b>14c</b>	PhCH <sub>2</sub>	<i>R</i>	20,060	>50,000	>50,000	>50,000
<b>14d</b>	PhCH <sub>2</sub>	<i>S</i>	833	20,730	2124	2076
<b>14e</b>	CH <sub>2</sub> (1-naphthyl)	<i>R,S</i>	229	6943	126	386
<b>14f</b>	CH <sub>2</sub> (2-naphthyl)	<i>R,S</i>	3492	>50,000	1392	1674
<b>14g</b>	CH <sub>2</sub> (3-indolyl)	<i>R</i>	2555	>50,000	2525	3506
<b>14h</b>	CH <sub>2</sub> (3-indolyl)	<i>S</i>	51	1157	35	49
<b>14i</b>	CH <sub>2</sub> (3-(7-azaindolyl))	<i>R,S</i>	107	481	74	63
<b>14j</b>	CH <sub>2</sub> (3-benzothienyl)	<i>S</i>	125	2545	60	223

Values are means of two experiments. IC<sub>50</sub> is quoted in nM.

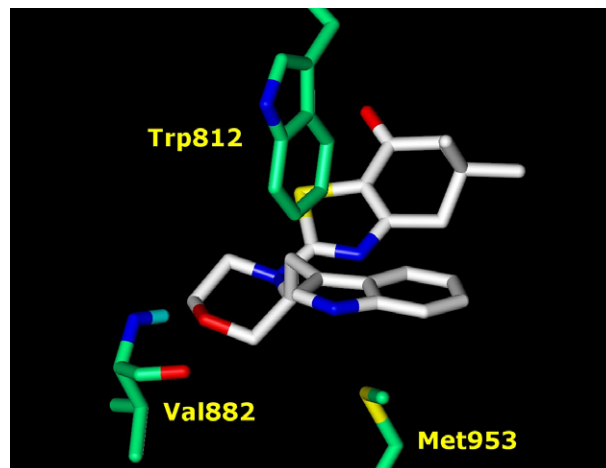
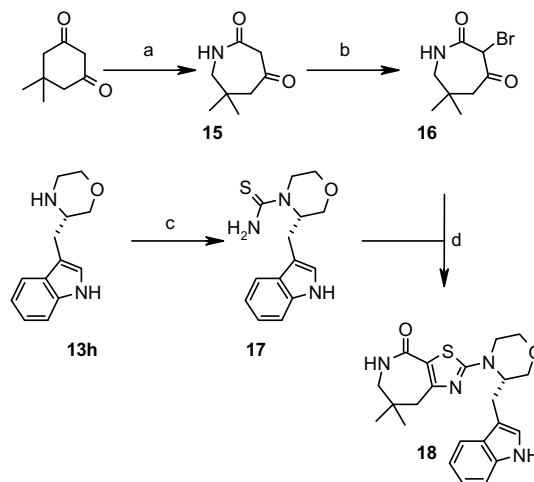


**Figure 3.** Docking of compound **14h** in the ATP site of PI3Kγ from 1E7V<sup>7</sup> using GOLD Version 3.2 (CCDC, Cambridge, UK).

The SAR of substitution on the morpholine ring is shown in Table 2.

Substitution of the morpholine ring with a phenyl group led to a loss in activity, compounds **14a** and **14b**. Introduction of a methy-



**Scheme 3.** Reagents and conditions: (a) NH<sub>2</sub>OH·HCl, pyridine, 4 Å molecular sieves, 25 °C; catalytic *p*-toluene sulfonic acid, pyridine, 65 °C, 65%; (b) NBS, NaHSO<sub>4</sub>, THF, 25 °C, 81%; (c) 1,1'-thiocarbonyldiimidazole, NH<sub>4</sub>OH, MeCN, 40 °C, 80%; (d) *i*-Pr<sub>2</sub>NEt, THF, reflux, 96%.

**Table 3**  
Potency in selected cell lines

Compound	pAKT <sup>S473</sup> (PC3)	Proliferation (PC3)	pAKT <sup>S473</sup> (MCF7)	Proliferation (MCF7)	Proliferation (U87-MG)
<b>1</b>	2939	5473	NT	IA	11,070
<b>14h</b>	1555	2840	NT	1255	787
<b>18</b>	1412	2066	199	862	3501

Values are means of two experiments. IC<sub>50</sub> is quoted in nM. NT, not tested; IA, inactive.

lene unit between the morpholine and the phenyl group lead to a differentiation in the activity of the enantiomers, the *R*, compound **14c**, being inactive and the *S*, compound **14d**, active. Replacing the phenyl by naphthyl showed a marked preference for the 1-substituted naphthyl, compound **14e**, over the 2-substituted, compound **14f**. The 1-naphthyl could be replaced by a 3-benzothieryl, 3-indolyl or 3-(7-azaindolyl), compounds **14j**, **14h**, and **14i**, respectively. There was a clear preference for the *S* enantiomer as shown by comparison of compounds **14h** and **14g** and supported by compounds **14d** and **14c**. Introduction of the morpholine substituent gives a degree of selectivity for PI3K $\alpha$ ,  $\delta$ , and  $\gamma$  over  $\beta$ . The increased potency of compound **14h** can be explained by Figure 3, which shows a docking of compound **14h** into the ATP binding site of PI3K $\gamma$ .<sup>7</sup> NMR data<sup>10</sup> suggest that the 3-substituent of the morpholine adopts an axial conformation. The lone pair of the morpholine oxygen of the ligand forms a hydrogen bond to the backbone NH of Val882. The indolyl substituent of the ligand projects toward solvent, closely fitting a space between a hydrophobic surface largely formed by the aliphatic side chain of Met953 below, and an edge-face  $\pi$ - $\pi$  stacking interaction with the indolyl side chain of Trp812 above.

Having identified the 3-indolyl methyl group as a substituent of interest, we sought to combine this with modification of the core scaffold. Reaction of **2** with hydroxylamine hydrochloride in pyridine followed by treatment with catalytic *p*-toluene sulfonic acid in pyridine gave the lactam **15** in 65% yield, which was converted to the bromide **16** with NBS in 81% yield. Morpholine **13h** was synthesized as shown in Scheme 2 from *S*-tryptophan and then converted to the thiourea **17** which was reacted with bromide **16** to give compound **18** in 96% yield (Scheme 3).

The lactam **18**<sup>11</sup> showed similar potency to the ketone **14h** against the PI3K isoforms (IC<sub>50</sub> = 59, 1006, 18, and 31 nM for  $\alpha$ ,  $\beta$ ,  $\delta$ , and  $\gamma$ , respectively).

Activation of the PI3K pathway leads to phosphorylation of Thr308 and Ser473 of AKT and subsequently a number of downstream substrates, including IKK, BAD, GSK, Forkhead, and Caspase-9. This activation triggers a range of responses in cell metabolism, cell death, cell cycle progression and cell differentiation. Hence, inhibiting PI3K should block phosphorylation of AKT and inhibit cell proliferation. Compounds **1**, **14h**, and **18** were profiled against PTEN negative PC3 prostate tumor and U87-MG glioblastoma cell lines and MCF7 breast cancer cells, a mutated PI3K $\alpha$  cell line, results shown in Table 3.

Compounds **14h** and **18** demonstrated the ability to inhibit the phosphorylation of AKT and inhibit proliferation via the PI3K pathway in PTEN negative and PI3K $\alpha$  mutant cell lines and were shown to be inactive against a panel of kinases that included AKT (data not shown). Compound **1** showed comparable activity to compounds **14h** and **18** in inhibiting the phosphorylation of AKT in PTEN negative cell lines. Compound **1** has similar potency to compounds **14h** and **18** against PI3K $\beta$  but is over twenty fold less active against PI3K $\alpha$ ,  $\delta$ , and  $\gamma$ , suggesting a role for PI3K $\beta$  in PTEN negative cell lines. However, compound **1** was inactive against the MCF7 cell line which has a PI3K $\alpha$  mutation reflecting the decreased activity against PI3K $\alpha$ ,  $\delta$ , and  $\gamma$ .

Compound **18** was selected over compound **14h** for in vivo pharmacokinetic profiling based on its superior solubility (com-

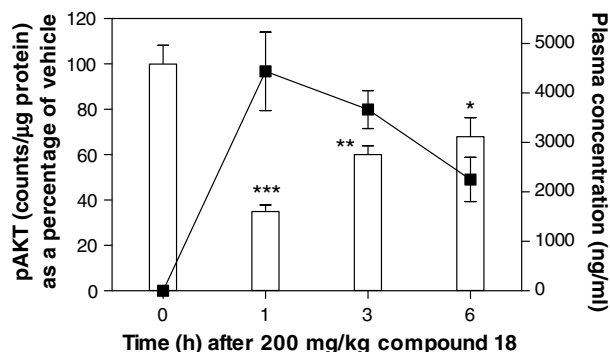


**Figure 4.** Time-dependent reduction of pAKT in U87-MG human glioma tumors after treatment with compound **18**. U87-MG tumor bearing mice were treated with vehicle (0 h), or 200 mg/kg compound **18** po. pAKT was measured by immunoassay in tumor homogenates at 1, 3, and 6 h post-treatment (bars). Drug plasma concentration was measured by LC-MS/MS (line). \*\*\**p* < 0.001%, \*\**p* < 0.01%, \**p* < 0.05% versus control, one-way ANOVA followed by Bonferroni post test.

pound **18** 642  $\mu$ M compared to compound **14h** 201  $\mu$ M, pH 7.4) and its lower in vitro intrinsic clearance (compound **18** 24  $\mu$ L/min/mg compared to compound **14h** 35  $\mu$ L/min/mg, male rat hepatocytes). The in vivo pharmacokinetics of compound **18** were assessed in female nude mice following single po administration at 30 mg/kg. Compound **18** had a C<sub>max</sub> of 1455 ng/mL at 1 h post dose and an AUC<sub>last</sub> of 2667 ng h/mL. Exposure increased at higher po doses and was deemed sufficient to progress compound **18** into xenograft studies.

The in vivo efficacy of compound **18** was assessed in nude mice bearing U87-MG tumors grown subcutaneously. Ex vivo analysis of tumor tissue after a single dose of 200 mg/kg po of compound **18** showed an inhibition of pAKT levels that was dependent on drug concentration, Figure 4. A 65% decrease in pAKT was observed at 1 h, and was partially sustained to 6 h (32% decrease compared to vehicle). Total AKT was also measured but stayed constant.

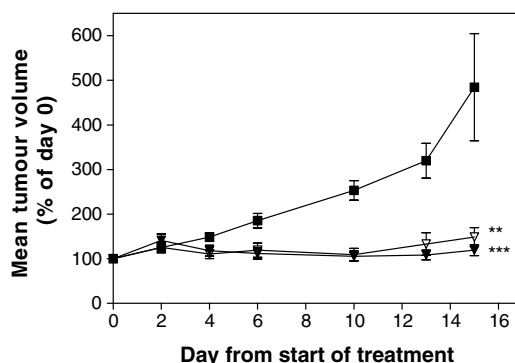


**Figure 5.** In vivo efficacy of compound **18** in U87-MG xenografts. U87-MG tumor bearing mice were treated with compound **18** po, twice per day for 14 days, at either 100 mg/kg (open triangles) or 200 mg/kg (closed triangles). The anti-tumor activity measured as optimum T/C % (mean volume of treated group divided by the mean volume of vehicle treated control group (closed squares), multiplied by 100) was 31% and 25% on day 15, respectively. \*\**p* < 0.01 versus control, \*\*\**p* < 0.001% versus control, two-way ANOVA followed by Bonferroni post test.

U87-MG tumor bearing mice were treated with compound **18** orally, twice per day for 14 days, achieving a *T/C* value of 31% on day 15 when dosed at 100 mg/kg po and a *T/C* of 25% on day 15 when dosed at 200 mg/kg po, Figure 5. There was no associated weight loss.

In conclusion a new series of PI3K inhibitors has been developed. These compounds show that inhibition of PI3K leads to blocking of phosphorylation of AKT and subsequent inhibition of proliferation in vitro. This effect is also demonstrated in vivo against cell lines in which the PI3K pathway is upregulated due to PTEN deletion, leading to reduced tumor growth in U87-MG xenograft models. Progress on improving in vivo efficacy of this promising series will be reported in due course.

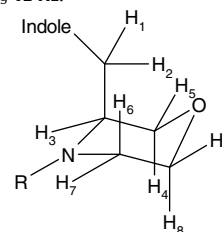
## Acknowledgments

We thank Jeff Kennedy for ITC measurements, Upasana Prabha-kar for cellular assays, Sarah Bartlett, Lloyd King, and Simon Carter for the in vivo PK studies, and Rachel Garlish for HR-MS data.

## References and notes

- (a) Vanhaesebroeck, B.; Leevers, S. J.; Panayotou, G.; Waterfield, M. *Trends Biochem. Sci.* **1997**, 22, 267; (b) Domin, J.; Waterfield, M. *FEBS Lett.* **1997**, 410, 91.
- (a) Ward, S. et al *Chem. Biol.* **2003**, 10, 207; (b) Ward, S. G.; Finan, P. *Curr. Opin. Pharmacol.* **2003**, 3, 426.
- Wymann, M. P. et al *Trends Pharmacol. Sci.* **2003**, 24, 366.
- (a) Brader, S.; Eccles, S. A. *Tumori* **2004**, 90, 2; (b) Samuels, Y. et al *Science* **2004**, 304, 554.

- Vivanco, I.; Sawyers, C. L. *Nat. Rev. Cancer* **2002**, 2, 489.
- Vlahos, C. J. et al *J. Biol. Chem.* **1994**, 269, 5241.
- Walker, E. H.; Pacold, M. E.; Perisic, O.; Stephens, L.; Hawkins, P. T.; Wymann, M. P.; Williams, R. L. *Mol. Cell* **2000**, 6, 909.
- Alexander, R. P.; Aujla, P.; Batchelor, M. J.; Brookings, D. C.; Buckley, G. M.; Crepy, K. V. L.; Kulisa, C. L.; Turner, J. P. WO 2006114606.
- Hopkins, A. L.; Groom, C. R.; Alex, A. *Drug Discovery Today* **2004**, 9, 430–431.
- Coupling constants ((CD<sub>3</sub>)<sub>2</sub>SO, 600 MHz, 100 °C) *J*<sub>1,2</sub> 14 Hz, *J*<sub>1,3</sub> 3.7 Hz, *J*<sub>2,3</sub> 11.0 Hz, *J*<sub>3,4</sub> 2.0 Hz, *J*<sub>3,5</sub> ca. 0.0 Hz, *J*<sub>4,5</sub> 11.6 Hz, *J*<sub>6,7</sub> 12 Hz, *J*<sub>6,8</sub> 12 Hz, *J*<sub>6,9</sub> 3.1 Hz, *J*<sub>7,8</sub> 3.0 Hz, *J*<sub>7,9</sub> 3.1 Hz, *J*<sub>8,9</sub> 12 Hz.



- Selected analytical data for compound **18**: <sup>1</sup>H NMR ((CD<sub>3</sub>)<sub>2</sub>SO, 600 MHz, 25 °C) δ 10.91 (d, 1H, *J* = 1.9 Hz), 7.81 (d, 1H, *J* = 7.8 Hz), 7.72 (t, 1H, *J* = 4.9 Hz), 7.35 (d, 1H, *J* = 7.8 Hz), 7.19 (d, 1H, *J* = 1.9 Hz), 7.09 (t, 1H, *J* = 7.8 Hz), 7.01 (t, 1H, *J* = 7.8 Hz), 4.11–4.06 (m, 1H), 3.98–3.92 (m, 1H), 3.71–3.66 (m, 1H), 3.62–3.55 (m, 1H), 3.51–3.48 (m, 1H), 3.55–3.46 (m, 1H), 3.45–3.35 (m, 1H), 3.28 (dd, 1H, *J* = 11.0 Hz, *J* = 13.8 Hz), 2.96–2.91 (m, 2H), 2.88 (dd, 1H, *J* = 4.1 Hz, *J* = 13.8 Hz), 2.73 (dd, 2H, *J* = 17.4 Hz, *J* = 17.4 Hz), 1.00 (s, 6H, CH<sub>3</sub>). <sup>13</sup>C NMR ((CD<sub>3</sub>)<sub>2</sub>SO, 75.5 MHz, 30 °C) δ 170.3, 164.3, 154.4, 136.7, 127.7, 124.1, 121.4, 118.9, 118.7, 118.0, 111.8, 110.7, 66.5, 65.9, 56.1, 51.9, 46.6, 43.8, 32.2, 26.7, 26.6, 23.2. Chiral purity: 98% ee, determined by HPLC using a CHIRALPAK AD 250 × 4.6 mm 10 μm column, HR-MS: Calcd for C<sub>22</sub>H<sub>27</sub>N<sub>4</sub>O<sub>2</sub>S<sup>+</sup>: 411.1855. Found: 411.1857.